Solution equilibrium behind the room-temperature synthesis of nanocrystalline titanium dioxide

4 AUTHORS:

Gulaim A Seisenbaeva
Swedish University of Agricultural Sciences
122 PUBLICATIONS **1,312** CITATIONS

Geoffrey Daniel
Swedish University of Agricultural Sciences
234 PUBLICATIONS **3,937** CITATIONS

Jean-Marie Nedelec
Ecole Nationale Supérieure de Chimie de Cl…
156 PUBLICATIONS **1,797** CITATIONS

Vadim Kessler
Swedish University of Agricultural Sciences
211 PUBLICATIONS **2,603** CITATIONS

Solution Equilibrium behind the Room-Temperature Synthesis of Nanocrystalline Titanium Dioxide

Gulaim A. Seisenbaeva,[‖,‡] Geoffrey Daniel,[‖] Jean-Marie Nedelec,[⊥,§] Vadim G. Kessler,*[‖,‡]

[‖] Department of Chemistry, Biocenter, Swedish University of Agricultural Sciences (SLU), Box 7015, SE-75007, Uppsala, Sweden, ‡ CaptiGel AB, Uppsala Science Park, 75183 Uppsala, Sweden, [⊥] Department of Forest Products/Wood Science, SLU, Box 7008, 75007 Uppsala, Sweden, [⊥] Clermont Université, ENSCCF, Institut de Chimie de Clermont-Ferrand, BP 10448, F-63177 Clermont-Ferrand, France, § CNRS, UMR 6296, ICCF, F-63171 AUBIERE, France

ABSTRACT: Formation of nanocrystalline and practically monodisperse TiO_2 from a water soluble and stable precursor, ammonium oxo-lactato-titanate, $(NH_4)_8Ti_4O_4(Lactate)_8 \cdot 4H_2O$, often referred to as TiBALDH or TALH, is demonstrated to be due to a coordination equilibrium. This compound, individual in the solid state, exists in solution in equilibrium with ammonium tris-lactato-titanate, $(NH_4)_2Ti(Lactate)_3$ and uniform crystalline TiO_2 nanoparticles (anatase) stabilized by surface-capping with lactate ligands. This equilibrium can be shifted towards nano-TiO_2 via application of a less polar solvents like methanol or ethanol, dilution of the solution, introduction of salts or raising the temperature, and reverted on addition of polar and strongly solvating media such as dimethyl sulfoxide, according to NMR. Aggregation and precipitation of the particles was followed by DLS and could be achieved by decrease in their surface charge by adsorption of strongly hydrogen-bonding cations, e.g. in solutions of ammonia, ethanolamine or amino acid arginine or by addition of ethanol. It might be this equilibrium that is via the same mechanism shifted towards nano-titania when organic polyelectrolytes, in particular, peptides and enzymes, are added to the medium.

INTRODUCTION

Crystalline nanoparticles of titania uniform in size and morphology have during recent years attracted tremendous and growing attention of researchers due to their application as constituents or building blocks for advanced materials in photocatalysis,[1,2] photovoltaics,[3,4] electrochemical water splitting and hydrogen production and storage,[5,7] in advanced adsorbents for separation of biomolecules particularly proteins,[8] for water remediation,[9,10] and even in bioencapsulation.[11,12] A large number of successful approaches have been developed for production of nano-titania including spray-pyrolysis,[13] chemical vapor- (CVD)[14] and atomic layer deposition (ALD),[15] and sol-gel[16] often combined with hydrothermal treatment to enhance crystallinity.[10,17,18] The increasing trend to improve sustainability and decrease energy cost in production of nanomaterials has driven special interest for identifying potential low cost, low risk and room temperature roots to oxide nanomaterials.[19] A solution to this quest has been the relatively recent discovery of techniques applying enzymes, proteins and polyelectrolyte polymers that are able to more-or-less rapidly transfer a cheap and commercially available water soluble and stable titanium precursor, formulated by providers as titanium(IV) bis(ammonium lactate)dihydroxide 50 wt% solution (Aldrich Cat. No 388165) often referred to as TiBALDH or TALH. This precursor has been found able to deliver impressively uniform (about 3 nm in size) fully crystalline (anatase or in some cases even rutile) nanoparticles via hydrothermal treatment,[20-22] but also in reactions with enzymes, medium chain (12-16 mer) peptides[23-25] or with ammonia, liberated from urea on heating[26] or through catalytic action of urease at room temperature.[27] A number of attempts has

been made to explain the molecular mechanisms of these processes.[22,25,27] These explanations were, unfortunately, questionable since they were not based on reliable information about the structure of the precursor or any true mechanistic investigations. In fact, the producers' formulation of this product as dihydroxide was highly controversial as the presence of two OH-ligands at the same Ti(IV) cation has never been observed in the structures determined so far according to Cambridge Crystallographic Data Centre (CCDC) and no structural characterization for this broadly used product was available. We have recently isolated TiBALDH in pure form by crystallization from commercially obtained solutions as rosette-shaped polycrystals, consisting of 0.5-0.6 mm long and less than 0.05 mm thick needles. Their X-ray powder pattern was indexed in a monoclinic unit cell with parameters a = 11.8685(2), b = 13.2396(2), c = 19.9578(2) Å, β = 107.718(3)°, Space group $P2_1/c$. The Rietveld refinement permitted to identify for this solid phase the Ti and O atom positions being in agreement with the core structure observed earlier for the oxo-oxalato-titanates,[28] see Fig. 1, and very close to that found in the structure of the oxo-peroxo-oxyacetato titanate.[29] These data, closely analogous to those in [28,29] even in the values of the unit cell parameters and the unit cell symmetry in combination with the EXAFS spectra, indicating Ti-O-Ti contacts, permitted us to formulate TiBALDH as tetrakis(di-lactato-oxo-titanate), $(NH_4)_8Ti_4O_4(Lactate)_8 \cdot 4H_2O$.[30]

The aim of the present paper was then to gain better insight in the structure and reactivity of this precursor in order to identify the pathways of its transformation into nano-TiO_2.
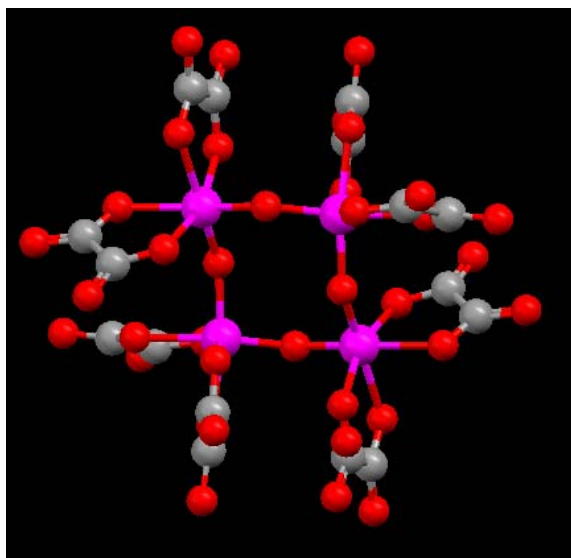
FIGURE 1 The molecular structure of the $Ti_4O_4(C_2O_4)_8^{8-}$·anion in the structures of Potassium titanium oxide oxalate dihydrate and Ammonium titanyl oxalate monohydrate (please, compare http://www.sigmaaldrich.com/catalog/product/aldrich/229989 and http://www.sigmaaldrich.com/catalog/product/sial/14007). The image is prepared with the ICSD Mercury software using the data from ref [28]. Titanium atoms are depicted in magenta, oxygen – in red, and carbon – in grey.

EXPERIMENTAL SECTION

Titanium(IV) bis(ammonium lactate)dihydroxide 50 wt% solution (Aldrich Cat. No 388165) was used directly as received in this work. The experiments were carried out with the freshly received samples and repeated with the product kept in a fridge at 3°C. No sign of change in appearance or reactivity could be observed even after 1 year of storage.

Single crystals of $(NH_4)_2[Ti(L-Lactate)_3]\cdot 3H_2O$ (**1**) were isolated in two types of experiments, the most productive being diluting fresh TiBALDH in 1:2 volume ratio with methanol or dissolving the polycrystals produced by air-drying in pure MeOH and letting the solution to evaporate slowly in air. The exact yield could not be determined because the TiO_2 powder formed as dense cake together with transparent plates (0.3-0.4 mm in average) of **1** that were forming a visibly massive precipitate. The other experiment consisted in dilution of the initial solution of TiBALDH 1:2 by distilled water and keeping it in a Teflon-clad autoclave at 160°C for 5 days. After cooling the product consisted of a solution with white precipitate on the bottom and a "collar" of small rhomb-shaped crystals on its surface also identified as **1** by X-ray single crystal study.

An attempt to crystallize a potassium analog of TiBALDH was carried by dissolution of solid KOH (0.22 g) in the undiluted industrial solution (50 wt %, 2 ml) and turned unsuccessful as the reaction solution dried out forming a transparent glassy solid. No precipitation of solid particles could be observed in this case.

The solution behavior of TiBALDH and the separated TiO_2 nanoparticles (for details, see below) was carried out with Bruker Avance HD 600 MHz spectrometer on ^1H and ^{13}C nuclei. Ligand exchange was followed by NOESY experiments. $H_2O:D_2O$ = 9:1 solutions were used for sample preparation.

The samples of TiBALDH were diluted 80 times. The portions of about 40 mg of non-dried nanoparticles separated by centrifugation were dispersed in 0.4 ml of the solvent by sonication.

Crystallography for 1. Crystal data for $C_9H_{26}N_2O_{12}Ti$: Hexagonal, Space Group P3, $a=b=$ 15.304(3), $c=$ 6.6665(13) Å, V = 1352.1(4) Å^3, d = 1.482 g/cm^3, μ = 0.534. 2142 [Rint = 0.0611] independent reflections were collected to 2θ < 58° using Bruker SMART Apex-II multipurpose diffractometer operating with MoKα radiation, λ = 0.71073 Å. The structure was solved by direct methods. All Atoms were located in the electron density map. The non-H atoms were refined anisotropically and H-atoms, found in the subsequent Fourier syntheses, only in isotropic approximation. All calculations were completed in Bruker Apex-II program package. Final discrepancy factors were R1 = 0.0345, wR2 = 0.0728.

Isolation and characterization of nano-TiO₂. The nanoparticle dispersions were produced by addition of 2 ml TiBALDH (50%) to 20 ml of 25% ammonia, 0.01 M KOH (pH = 12), 5 wt % ethanolamine, $HOC_2H_4NH_2$, 5 wt% arginine, $C_6H_{14}N_4O_2$, 1M NaCl and 1M AlCl₃ to pure water and to 96% ethanol. The phase separation of the particles was followed by visual observation and by DLS measurements using Malvern Zeta-sizer instrument. In the cases, where opalescence could be observed by bare eye, the produced particles were separated by centrifugation at 4000 rpm for 15 min. The X-ray powder patterns were recorded for the gel-like centrifugates put into a glass capillary (Lindeman tube) on the multipurpose Bruker Apex-II diffractometer operating with MoKα radiation. Bruker Apex-II and Eva software were used for integration and data treatment.

The particles were alternatively washed twice with ethanol and dried in air. They were investigated by high resolution transmission electron microscopy (HRTEM) using a Philips CM-20 Super Twin microscope, operating at 200 kV. Samples for HRTEM were prepared by dispersing a powder in methanol and leaving a droplet of the suspension on a copper microscope grid covered with perforated carbon. Elemental analysis was carried out using a SEM-EDS Hitachi TM 1000-μDeX Tabletop Microscope. Size distribution of the particles redistributed in ethanol by sonication was measured with Nanoparticle Tracking Analysis NanoSight LM10 HSB instrument for 90 s. The instrument calibration was carried out using polystyrene latex beads with the size 100 nm.

RESULTS AND DISCUSSION

Solid state structure of the molecular reaction product. In an aim to provide more in-depth understanding of the structure and reactivity of TiBALDH, we decided to produce single crystal structure data for this compound, which would allow to locate the hydrogen bonds in its structure and to identify active sites for potential molecular reactivity. Obtaining single crystals of this compound from water solutions is practically impossible as it easily forms highly viscous supersaturated solutions and even glassy solids in which rosette-shaped polycrystals slowly appear on storage. We then decided to produce single crystals through re-dissolution of the polycrystalline product in a less viscous and less polar (and less efficiently hydrogen bonding) solvent such as methanol. The solid, obtained by drying of TiBALDH dissolved readily in MeOH, producing fully transparent and clear yellowish solutions. Their slow evaporation under ambient conditions provided platelet transparent colorless crystals embedded in a

white non-transparent solid. This product was readily re-dissolvable in both methanol and water. The single crystal X-ray study of the transparent crystals showed them unexpectedly to be a new phase of ammonium tris-lactato-titanate trihydrate, $(NH_4)_2[Ti(L-Lactate)_3]\cdot 3H_2O$ (Fig. 2). It should be noted that crystals of the same compound have been isolated from the hydrothermal synthesis of TiO_2 from TiBALDH according to [21], which we reproduced.

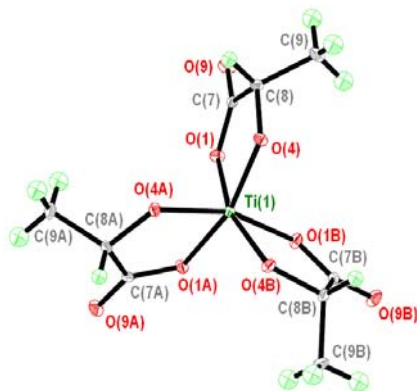FIGURE 2. Molecular structure of one of the three $[Ti(Lactate)_3]^{2-}$ anions in the unit cell of the structure of $(NH_4)_2[Ti(L-Lactate)_3]\cdot 3H_2O$ (**1**).

The structure of the tris-lactato complex reported here differs from the structure of $(NH_4)_2[Ti(L-Lactate)_3]$ reported earlier by Kakihana et al.,[31] by the presence of 9 water molecules per unit cell involved into H-bonding. This difference leads to a more dense packing in the crystal structure which in this case is hexagonal (trigonal) non-centrosymmetric and achiral (space group P3) in contrast to chiral cubic structure (space group $P2_13$) observed earlier for water-free $(NH_4)_2[Ti(L-Lactate)_3]$. Each Ti-atom is placed on the 3-fold axis and is attached to a single symmetrically independent ligand. The H_2O-molecules are involved together with ammonium ions in hydrogen bonding to the anions.
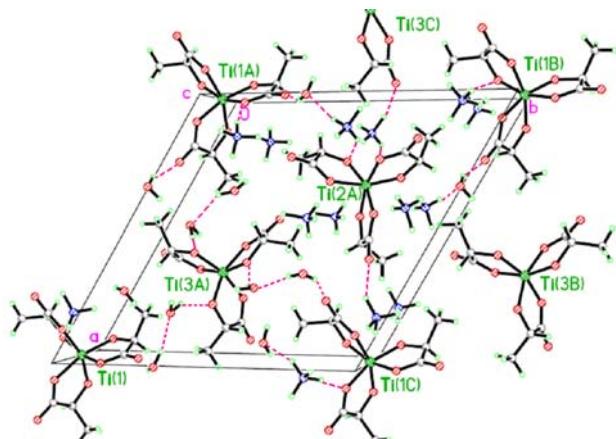

FIGURE 3 Unit cell of **1** with indication of the principal hydrogen bond motifs (dotted lines in magenta. For details, please, see Tab. TS6).

The dominating motif is the hydrogen bonding to the alkoxide oxygen atoms of the lactate anions (see Fig. FS1 and Tab. TS1-TS6), together with the bonding to single-bonded car-

boxylate oxygen atoms (connected to the Ti(IV) center). The hydrogen bonding to the double bonded carboxylate oxygen atom is rare in this structure (1 of 14 crystallographically independent hydrogen bonds). This indicates that the molecular mechanism of hydrolysis should be dominated for lactate (semi-alkoxide) complexes by proton-assisted S_N1 reactions – otherwise the usual pathway for alkoxide precursors, that would occur extremely rapidly at lower pH (below 3, ca. one pH-unit below the pKa for the lactic acid).[32]

Identification of the reaction pathway. In order to understand the transformation of $[Ti_4O_4(Lactate)_8]^{8-}$-anions in methanol, we used TEM to study the whole transparent methanol solution of dried TiBALDH containing a mixture of tris-lactate complex and white non-transparent matter placed on formvar coated copper grids.
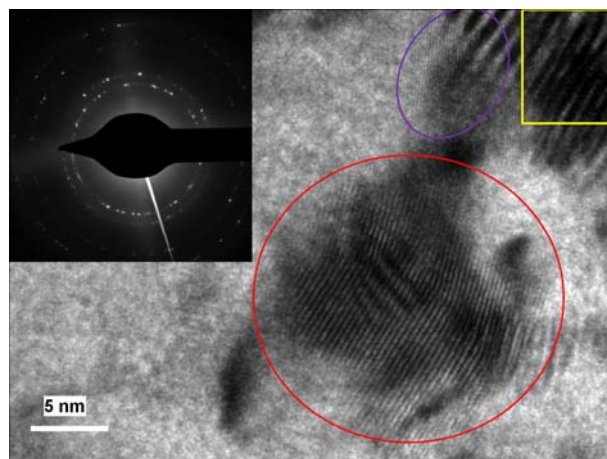

FIGURE 4. TEM micrographs and selected area electron diffraction (SAED) of the sample produced by drying of a solution of TiBALDH in methanol. Red circle shows anatase in 1 0 1 and violet circle in 0 0 1 orientation (0.35 and 0.20 nm fringes respectively). The yellow rectangle shows amorphous lamellar structure produced by decomposition of the metal-organic phase $((NH_4)_2[Ti(L-Lactate)_3]\cdot 3H_2O)$.

This work clearly showed that the solution already contained well-defined crystalline TiO_2 nanoparticles (anatase) (see Fig. 4 and FS2, FS3), together with a metal-organic phase that decomposed under the electron beam with formation of amorphous lamellar structures. The poorly defined black lines (like in the middle of the Fig. 4) are most probably Moire fringe patterns in overlapping nanocrystals, but there are also numerous better defined lamellar fragments like that in the yellow rectangle in the same figure. The nano- and submicron size lamellar structures have been demonstrated as products of both hydrolytic[33] and thermolytic[34] decomposition of metal-organic precursors. The TiO_2 particles in this case were visibly aggregated, supposedly, because of the intermediate drying step. The polarity and capacity of methanol to hydrogen bonding are high enough to insure their transfer into colloid solution.

It was then logical to use an even less polar and less efficient hydrogen bonding solvents such as ethanol. Addition of 1 ml of TiBALDH to ca. 20 ml 96% C_2H_5OH caused immediate precipitation of an extremely fine white powder which was isolated by centrifugation and identified by XRD as practically phase-pure anatase with particle size of ca 3 nm according to Debye-Scherrer calculation. After re-distribution in solution

3

by sonication, the particles showed an aggregate size of 100-200 nm according to NanoSight data. $(NH_4)_2[Ti(L-Lactate)_3] \cdot 3H_2O$ has been isolated on air drying of the corresponding supernatant. What is especially exciting is that this reaction is easily and equally rapidly reverted by addition of about the same or larger volume of water (please, see real time movie in the Supplementary). This reveals that TiBALDH actually exists continuously in solution in equilibrium with the tris-lactato titanate and TiO_2 nanoparticles.

$$3[Ti_4O_4(Lactate)_8]^{8-} + 8NH_4^+ \rightleftharpoons 8[Ti(Lactate)_3]^{2-} + 4TiO_2$$
$$+ 8NH_3 + 4H_2O \ (1)$$
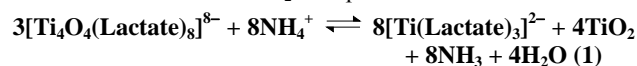
SCHEME 1 Coordination equilibrium describing formation of TiO_2 nanoparticles from TiBALDH

It has to be mentioned that this equilibrium according to equation (1) is associated with evolution of ammonia that can evaporate and in this way promote the shift towards titania nanoparticles and the compound (**1**). It means that the nanoparticles can spontaneously be generated in solution on storage if the vessel with the precursor solution is not closed properly and not stored at lower temperature.

Precipitation of crystalline TiO_2 nanoparticles apparently results from the shift of the equilibrium shown in Scheme 1 toward the colloid solution. Rapid re-dissolution of nano-titania in the presence of lactate and oxalate ligands is not as peculiar as it might seem in the view that solutions of these ligands are employed in leaching of titanate ores[35] dissolving even bulk TiO_2. The kinetics of dissolution of 3 nm TiO_2 particles in a citrate buffer pH = 6.5 with different citrate concentrations is reported in [36]. The pH dependence of etching of the aggregates of 4 nm TiO_2 nanoparticles by citrate solutions is reported in [37]. Quantitative dissolution of TiO_2 freshly precipitated from an alkoxide precursor (particle size about 5 nm) with formation of an analog to TiBALDH is described in [38].

Solution equilibrium studies by NMR. The ^1H and ^{13}C spectra of TiO_2 nanoparticles precipitated from TiBALDH by addition of ethanol, washed several times by EtOH and re-dispersed in water by sonication, have displayed a distinct combination of signals being a fingerprint of lactate anions. The ^1H spectrum shows a quadruplet at 4.01 ppm (1H, C*H*) and a doublet at 1.23 ppm (3H, C*H$_3$*), see Fig. 6, very close to the signals of commonly observed lactate species.[39]

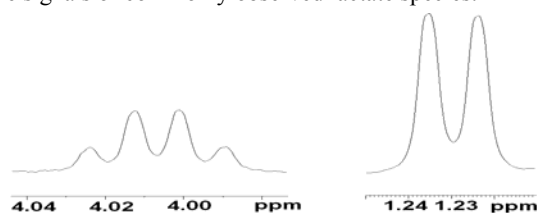
FIGURE 6. ^1H spectrum of the re-dispersed nano-TiO_2 produced from TiBALDH, demonstrating retention of lactate ligands (referenced to the H_2O signal).

The spectra of TiBALDH are really interesting. First of all, they always contain traces of iso-propanol (see FS 10, indicating that this product is most probably obtained via recovery of wastes in production of titanium alkoxide, the tetra-isopropoxide, TTIP, by a technique analogous to that described in [38]). In both ^1H and ^{13}C spectra of TiBALDH are present two rather different sets of lactate signals. One is quite close to that reported by Kakihana et al.[31] for the $[Ti(L-Lactate)_3]^{2-}$ and characterized by relatively high chemical

shifts (see Fig. 7), in particular, 4.96 ppm (compare with about 5 ppm in [31]) for the ^1H C*H*-signal. The other is closer to the commonly observed ionic lactate, but with the energy gap between C*H* and C*H$_3$* signals significantly shortened compared to the lactate spectrum for the species observed on the surface of TiO_2 in the present work (1659 Hz compared to 1665 Hz). This indicates that this set of signals originates most probably not from a single type of ligand, but from quick exchange between at least two ones, in this case apparently the oxo-lactate and lactate-capped $TiO2$ having very close chemical shifts.
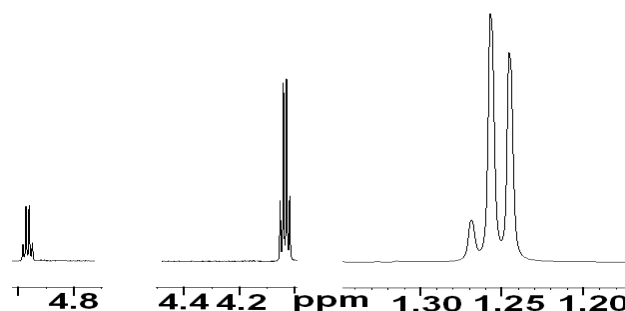

FIGURE 7. ^1H spectrum of TiBALDH diluted 80 times by H_2O-D_2O solution (referenced to the H_2O signal).

Unequivocal evidence for the exchange phenomenon can be obtained from Nuclear Overhauser enhancement spectroscopy (NOESY), where correlation signals emerge when spins are transferred between the atoms coming into proximity of each other.[40]
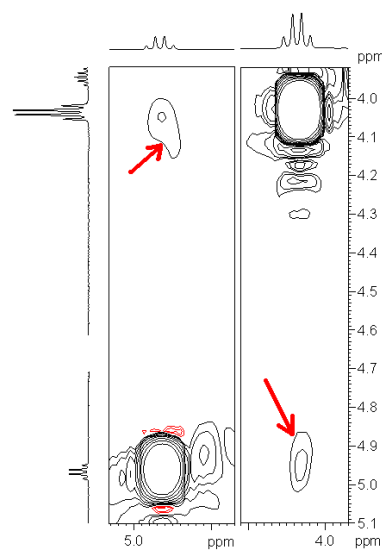

FIGURE 8. Fragment of NOESY spectrum of diluted TiBALDH in the lactate C*H* region showing correlations signals (indicated by red arrows) for the ligand exchange between $[Ti(Lactate)_3]^{2-}$, and oxo-lactate/lactate capped nano-TiO_2.

The spectrum shown in the Fig. 8 (water signal is omitted for clarity, full spectrum is shown in FS11) displays undeniably the exchange between both observed lactate C*H*-signals, corresponding to $[Ti(L-Lactate)_3]^{2-}$ and oxo-lactate/lactate-capped titania. The NOESY spectra display also strong correlation signals between both C*H* and the partly overlapping C*H$_3$*-signals (see Fig. 9), which originate in the first hand due to proximity of the H-atoms in the neighboring CH and CH_3 in

4

each type of lactate. The Overhauser effect here is negative for the signal from tris-lactate, but positive for that from oxo-lactate – a possible indirect indication of the lower solution mobility or higher molecular weight of the species bearing this ligand.[41]
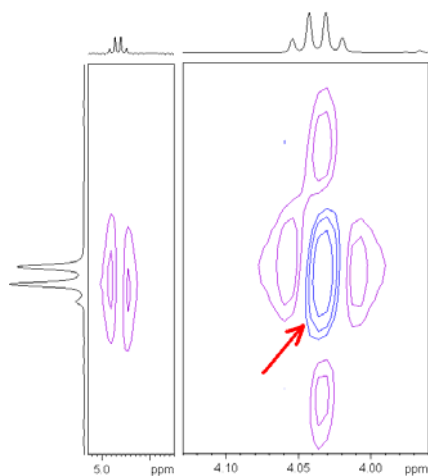

FIGURE 9. Fragment of NOESY spectrum of diluted Ti-BALDH showing signals for C*H*-C*H*$_3$ correlations for the ligand exchange between [Ti(L-Lactate)$_3$]$^{2-}$, and oxo-lactate/lactate capped nano-TiO$_2$. Positive Overhauser effect (blue signal) is indicated by red arrow.
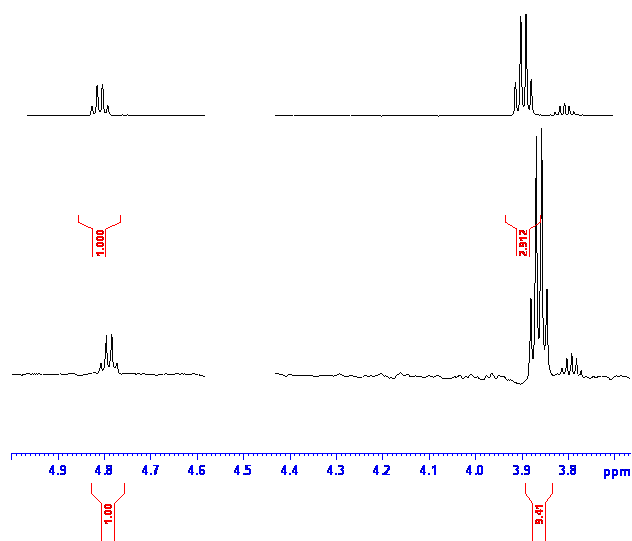

FIGURE 10. Integrated lactate C*H*-signals for diluted TiBALDH solution (above) and the same solution with 5 vol% (CH$_3$)$_2$SO added (below). The spectra are referenced to the C*H*$_3$-shift of (CH$_3$)$_2$SO taken as 2.503 ppm.

^{1}H NMR provides an excellent possibility also to follow the equilibria quantitatively. The ratio between the two C*H*-signals is an indicator of the equilibrium shift in the equation (1). Logically, less polar solvents are shifting the equilibrium to the right, resulting in less polar [Ti(L-Lactate)$_3$]$^{2-}$ and ultimately – the precipitation of titania. Addition of more polar and especially strongly solvating agents shifts it, on the contrary back towards the oxo-lactate complex. Thus while Ti-BALDH diluted 80 times shows 1:2.91 ratio between lactate in tris-lactate complex and in oxo-lactate/lactate-capped titania

(mostly, of course, oxo-lactate), the addition of 5 vol% of dimethyl sulfoxide (polarity 7.2, hard solvating factor HDs = 37.8 compared to 24.7 for water[42]) immediately changes the ratio into 1:9.41, i.e. converts about 2/3 of the tris-lactate together with nanoparticles into the original oxo-lactate.

Investigation of factors influencing the equilibrium by DLS. Taking into account that the discovered equilibrium was involving colloid solid particles of titanium dioxide, it appeared interesting to test influence of the common factors used in colloid chemistry, such as dilution, application of a different solvent and the solutions of salts to see, whether they can influence this process. The surface charge of titania particles is strongly influenced by such factors as pH and especially by ionic strength with the isoelectric point changing from as low as below pH = 2 for lower ionic strength to pH = 6.25 for high ionic strength.[43] Merck high purity water (pH = 7.0) was used to dilute the solutions that were prepared by addition of 2 ml TiBALDH to 20 ml of 25% ammonia, 0.01 M KOH (pH = 12), 5 wt % ethanolamine, HOC$_2$H$_4$NH$_2$, 5 wt% arginine, C$_6$H$_{14}$N$_4$O$_2$, 1M NaCl and 1M AlCl$_3$, 99.5% MeOH and pure water. The transformations were followed by both visual observation and DLS measurements.

The appearance of opalescence and precipitation of TiO$_2$ occurred in the order: 25% NH$_3$ (pH = 12.3) > 5% arginine (pH = 11.2) > 5% ethanolamine (pH = 11.7) >> 0.01 M KOH (pH = 12.0). The solutions of electrolytes, NH$_4$Cl, NaCl and AlCl$_3$, as well as those in pure water and in methanol showed no opalescence but did contain well defined non-aggregated nanoparticles with sizes 3-4 nm according to DLS for pure water, NH$_4$Cl, pH = 4.6, and AlCl$_3$, pH = 2.5, and with low degree of aggregation in pH-neutral solutions of NaCl and MeOH (see Fig. 11). It is important to note that the non-diluted 50 wt% TiBALDH does not reveal the presence of dissolved nanoparticles in any considerable amounts.
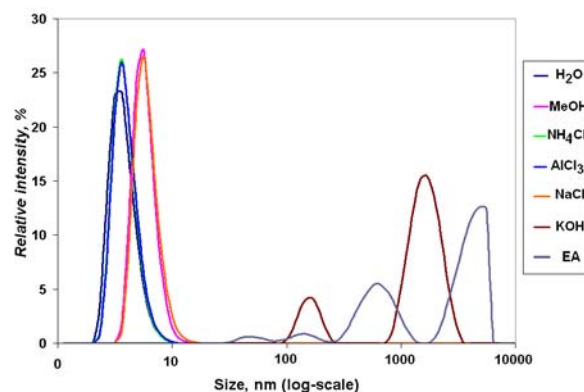

FIGURE 11. Size distribution for TiO$_2$ nanoparticles produced by dilution of 50 wt% TiBALDH by water (black), NH$_4$Cl solution (green), AlCl$_3$ solution (blue), methanol (pink), KOH (brown) and ethanolamine (grey).

Precipitation of TiO$_2$ from NH$_3$ and arginine was practically quantitative according to Scheme 1 after 30 h. This indicates clearly that the observed process of precipitation is not related to hydrolysis (in the view of limited ceramic yield and apparent independence of pH – in the concentrated KOH solution no precipitation could be observed at all). The X-ray diffraction for NH$_3$-derived material showed a considerable content of the hydrated H$_2$TiO$_3$ phase (Fig. 12b, c), indirectly confirming the role of hydrogen bonding during its formation.
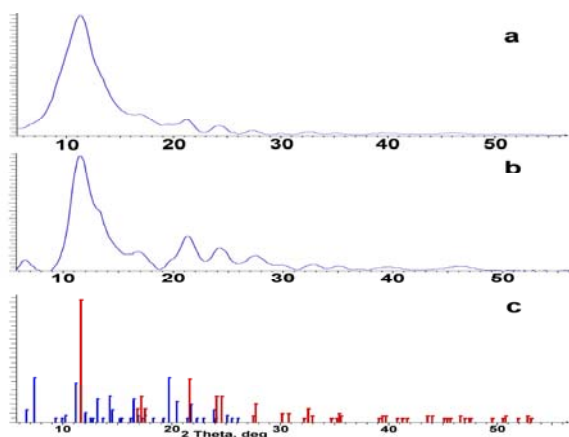
5

FIGURE 12. XRD of TiO$_2$ precipitated from TiBALDH by ethanol (a), 25% NH$_3$ (b) and the reference patterns of anatase, red, and H$_2$TiO$_3$, blue (c).

It is interesting to note that when 2 ml of TiBALDH are added to 20 ml of a saturated NaCl solution at room temperature, there is no opalescence and the solution is stable. However, if it is set to boiling, the TiO$_2$ precipitates from it, but re-dissolves readily on cooling to the room temperature again.

CONCLUSIONS

The obtained data indicate unequivocally that formation of nano-TiO$_2$ from TiBALDH can be achieved exploiting a coordination equilibrium of ligand redistribution that can be successfully shifted in both directions by simple means of changing polarity of the solvent or addition of salts. This phenomenon offers crystalline product already at room temperature. In the view that this equilibrium occurs at a variety of conditions, including neutral pH and room temperature, it might be supposed that it may also stay behind the synthesis of titania from the same precursors involving organic polyelectrolytes, in particular, peptides and enzymes.

ASSOCIATED CONTENT

Supporting Information. Crystallographic data in cif and table format, detailed description of hydrogen bonding in (NH$_4$)$_2$[Ti(L-Lactate)$_3$]·3H$_2$O, additional TEM images, DLS data on particle size in solutions and NanoSight data on particle size distribution, photos of produced TiO$_2$ colloids, details of NMR experiments and a real-time movie demonstrating the equilibrium leading to TiO$_2$ formation and re-dissolution in pH-neutral ammonium lactate solutions. This material is available free of charge via the Internet at http://pubs.acs.org.

AUTHOR INFORMATION

Corresponding Author

Vadim.Kessler@slu.se

Author Contributions

The manuscript was written through contributions of all authors. / All authors have given approval to the final version of the manuscript.

ABBREVIATIONS

MeOH, methanol; EtOH, ethanol; XRD, X-ray powder diffraction; NOESY, Nuclear Overhauser enhancement spectroscopy.

REFERENCES

(1) Di Paola, A.; Garcia-Lopez, E.; Marci, G.; Palmisano, L. *J. Hazard. Mater.* **2012**, *211*, 3.

(2) Zhang, C.B.; Liu, F.D.; Zhai, Y.P.; Ariga, H.; Yi, N.; Liu, Y.C.; Asakura, K.; Flytzani-Staphanopoulos, M.; He, H. *Angew. Chem.* **2012**, *51*, 9628.

(3) O'Regan, B.; Grätzel, M. *Nature* **1991**, *353*, 737.

(4) Hagfeldt, A.; Boschloo, G.; Sun, L.C.; Kloo, L.; Pettersson, H. *Chem. Rev.* **2010**, *110*, 6595.

(5) Anta, J.A. *Current Opinion Colloid Interface Sci.* **2012**, *17*, 124.

(6) Sun, C.H.; Liu, L.M.; Selloni, A.; Lu, G.Q.; Smith S.C. *J. Mater. Chem.* **2010**, *20*, 10319.

(7) Schlapbach, L.; Zuttel, A. *Nature* **2001**, *414*, 353.

(8) Ma, W.F.; Zhang, Y.; Li, L.L.; You, L.J.; Zhang, P.; Zhang, Y.T.; Li, J.M.; Yu, M.; Guo, J.; Lu, H.J.; Wang, C.C. *ACS Nano* **2012**, *6*, 3179.

(9) Luo, T.; Cui, J.L.; Hu, S.; Huang, Y.Y.; Jing, C.Y. *Env. Sci. Tech.* **2010**, *44*, 9094.

(10) Seisenbaeva, G.A.; Daniel, G.; Nedelec, J.M.; Gun'ko, Y.K.; Kessler, V.G. *J. Mater. Chem.* **2012**, *22*, 20374.

(11) Kessler, V.G.; Seisenbaeva, G.A.; Håkansson, S.; Unell, M *Angew. Chem.* **2008**, *47*, 8506.

(12) Yang, S.H.; Ko, E.H., Choi, I.S. *Langmuir* **2012**, *28*, 2151.

(13) Peng, B.; Jungmann, G.; Jager, C.; Haarer, D.; Schmidt, H.W.; Thelakkat, M. *Coord. Chem. Rev.* **2004**, *248*, 1479.

(14) Dunnill, C.W.; Kafizas, A.; Parkin, I.P. *Chem. Vapor Dep.* **2012**, *18*, 89.

(15) Meng, X.B.; Yang, X.Q.; Sun, X.L. *Adv. Mater.* **2012**, *24*, 3589.

(16) Livage, J.; Sanchez, C.; Henry, M.; Doeuff, S. *Solid State Ionics* **1989**, *32-33*, 633.

(17) Nilsson, E.; Sakamoto, Y.; Palmqvist, A.E.C. Chem. Mater. **2011**, 23, 2781-2785.

(18) Yu, J.G.; Su, J.R.; Cheng, B. *Adv. Funct. Mater.* **2007**, *17*, 1984.

(19) Dickerson, M.B.; Sandhage, K.; Naik, R.R. *Chem. Rev.* **2008**, *108*, 4935.

(20) Möckel, H.; Giersig, M.; Willig, F. *J. Mater. Chem.* **1999**, *9*, 3051.

(21) Matolygina, D.A.; Baranchikov, A.E.; Ivanov, V.K.; Tretyakov, Y.D. *Doklady Chem.* **2011**, *441*, 361.

(22) Kinsinger, N.M.; Wong, A.; Li, D.S.; Villalobos, F.; Kisailus, D. *Cryst. Growth Design* **2010**, DOI: 10.1021/cg101105t

(23) Kröger,N.; Dickerson, M.B.; Ahmad, G.;Cai, Y.; Haluska, M.S.; Sandhage, K.H.; Poulsen, N.; Sheppard V.C. *Angew. Chem.* **2006**, 118, 7397.

(24) Dickerson, M. B.; Jones, S. E.; Cai, Y.; Ahmad, G.; Naik, R. R.; Kröger, N.; Sandhage, K. H. *Chem. Mater.* **2008**, *20*, 1578.

(25) Zhao, C.X.; Yu, L.; Middelberg, A.P.J. *RSC Adv.* **2012**, *2*, 1292.

(26) Lee, S.W.; Sigmund, W.M. *Chem. Comm.* **2003**, 780.

(27) Johnson,J.M.; Kinsinger, N.; Sun, C.; Li, D.S.; Kisailus, D. J. Amer. Chem. Soc. 2012, DOI: 10.1021/ja306884e

(28) Fu, Y.L.; Liu, Y.L.; Shi, Z.; Li, B.Z.; Pang, W.Q. J. Solid State Chem. **2002**, *163*, 427

(29) Tomita, K.; Petrykin, V.; Kobayashi, M.; Shiro, M.; Yoshimura, M.; Kakihana, M. *Angew.Chem., Int.Ed.* **2006**, *45*, 2378.

(30) Groenke, N.; Seisenbaeva, G.A.; Kaminsky, V.V.; Zhivotovsky, B.; Kost, B.; Kessler, V.G. *RSC Adv.* **2012**, *2*, 4228.

(31) Kakihana, M.; Tomita, K.; Petrykin, V.; Tada, M.; Sasaki, S.; Nakamura, Y. *Inorg.Chem.* **2004**, *43*, 4546.

(32) Kessler, V.G.; Spijksma, G.I.; Seisenbaeva, G.A.; Håkansson, S, Blank, D.H.A; Bouwmeester, H.J.M *J. Sol-Gel Sci. Tech.* **2006**, *40*, 163.

(33) Seisenbaeva, G.A.; Daniel, G.; Nedelec J.M.; Kessler, V.G. *J. Mater. Chem.* **2012**, *22*, 20374.

(34) Nunes, G.G.; Seisenbaeva, G.A.; Kessler, V.G. *Cryst. Growth Design* **2011**, *11*, 1238.

(35) Corbin, D.R.; Griffin, T.P.; Hutchenson, K.W.; Li, S.; Shiflett, M.B.; Torardi, C.; Zaher, J.J. US Pat 8,137,647.

(36) Kessler, V.G., Seisenbaeva, G.A.; Håkansson, S.; Unell, M. *Angew. Chem. Int. Ed.* **2008**, *47*, 8506.

(37) Mudunkotuwa, I.A.; Grassian, V.H J. Amer. Chem. Soc. **2010**, *132*, 14986.

(38) Hardy, A.; D'Haen, J.; Van Bael, M.K.; Mullens, J. *J. Sol-Gel Sci. Tech.* **2007**, *44*, 65.

(39) Lloyd, S.G.; Zeng, H.; Wang, P.; Chatham, J.C. *Magn.. Reson. Med.* **2004**, *51*, 1279.

(40) Anet, F.A.L.; Bourn, A.J.R. *J. Amer. Chem. Soc.* **1965**, *87*, 5250.

(41) Bell, J R.A.; Saunders K. *Can. J. Chem.* **1968**, *46*, 3421.

(42) Persson, I. *Pure Appl. Chem.* **1986**, *58*, 1153.

(43) Preocanin, T.; Kallay, N. .*Croatica Chem. Acta* **2006**, *79*, 95.

Ammonium oxo-carboxylato-titanates display equilibrium with tris-carboxylate species and crystalline nano-TiO$_2$. It can be shifted in both directions varying polarity of the solvents and influencing the colloid stability of produced nano-titania.

TiBALDH / TALH   (NH$_4$)$_2$[Ti(D,L-Lactate)$_3$]   nano-TiO$_2$